INVESTIGATING CLIMATE FORCINGS RECORDED IN TROPICAL ICE CORES

2006 NASA Graduate Student Summer Program

Natalie Kehrwald
Byrd Polar Research Center
The Ohio State University
1060 Carmack Road
Columbus, OH 43210
kehrwald.1@osu.edu

Advisor: Dr. Gavin Schmidt
Goddard Institute for Space Studies
2880 Broadway
New York, NY 10025
gschmidt@giss.nasa.gov

1. INTRODUCTION

South Asia is the most densely populated area of the world, and previous monsoon failures have accounted for some of the worst famines in human history. The unprecedented rate of warming in the twentieth century means that people living in South Asia cannot establish their ability to adapt to changes in the monsoon based on what they have known in their lifetime. Temporal and spatial variations in temperature and precipitation are catalogued in Tibetan cores collected by the Ice Core Paleoclimatology Group at Byrd Polar Research Center (BPRC) at The Ohio State University (OSU). Ice cores offer records of past atmospheric chemistry, humidity, volcanic activity, solar activity, wind speed and tropospheric turbidity. The Dasuopu core (28º23'N, 85º43' E) provides a high resolution record of South Asian monsoonal moisture (Thompson et al., 2000) and may document monsoon failure due to both anthropogenic forcing and natural climate variability.

General circulation models (GCMs) incorporate the dynamical processes that determine climate, including interactions between the ocean, atmosphere, and sea ice. Models provide a horizontal analysis of climate that a single proxy record cannot supply. The degree to which the Dasuopu ice core and the GISS ModelE can reproduce similar climate conditions increases our confidence both in the model and in the proxy record. This study uses ModelE to recreate the complexities of the climate system acting upon the isotopes in precipitation archived in ice cores. Dasuopu data is correlated to sea surface temperatures, surface air temperatures, and deuterium in water vapor at 500 hPa. The seasonal effects of the monsoon and westerlies on Tibetan ice cores are also investigated. The comparison of paleoclimate proxy data with GCMs provides a more integrated interpretation of the climate system than when either method is analyzed separately.

2. PREVIOUS WORK

2.1 Regional Ice Core Composites

The BPRC Ice Core Paleoclimatology Group has collected cores from Africa, Antarctica, Bolivia, China, Greenland, Peru, Russia, and the United States. Tropical ice cores provide continental paleoclimate data from locations where few other proxy records exist. Due to their high accumulation rates, tropical ice cores provide high-resolution records for the mid- to late-Holocene. The relative proximity of tropical cores to human activity allows them to record the anthropogenic alteration of the climate system. Regional composites have recently been compiled for the Andean and Tibetan ice cores (Figures 1 and 2). The integration of individual cores into a regional record allows for spatial climate analysis through time (Thompson et al., 2006).

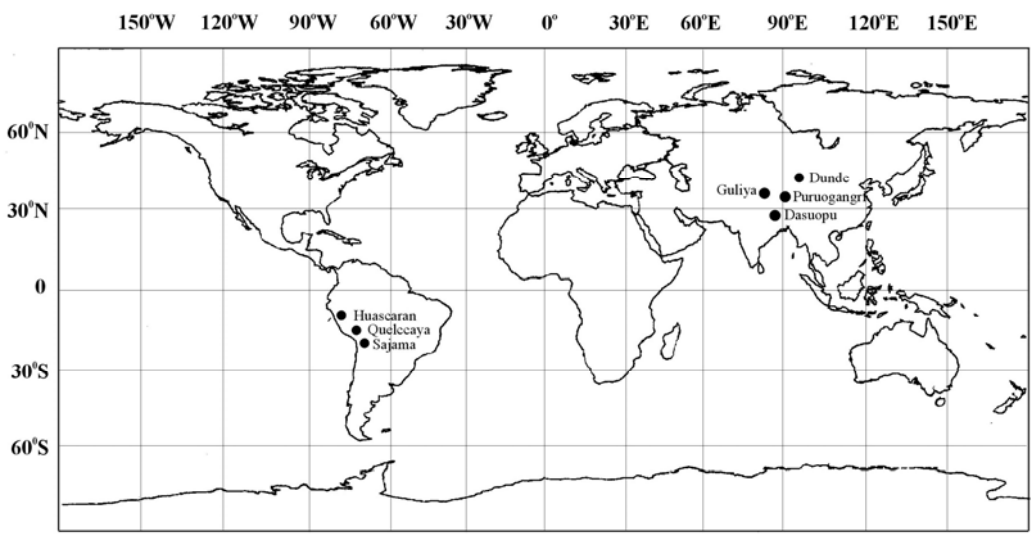

Figure 1: Location of BPRC ice cores mentioned in the text.

Air temperature at the time of condensation is recorded in the oxygen isotope ratios ($\delta^{18}O$) of the ice core (Thompson et al., 2005). The amount of snow accumulation on the ice cap is a proxy for precipitation. Because the weight of the overlying layers compresses and thins the ice below, annual net accumulation is determined by flow models that incorporate ice thickness, average accumulation rate, and ice equivalent depth (Bolzan, 1985; Davis et al., 2005; Thompson et al., 1998). Most tropical precipitation falls during the warm, wet summer season. The Andean cores are all located in the Southern Hemisphere, while the Tibetan cores are Northern Hemisphere records. The Andean and Himalayan composites

therefore also provide a comparison of Northern and Southern Hemisphere summer temperature and precipitation (Thompson et al., 2006). The Tibetan and South American cores both depict an exponential temperature rise in the second half of the twentieth century which correlates with observed temperature values (Jones et al., 1999).

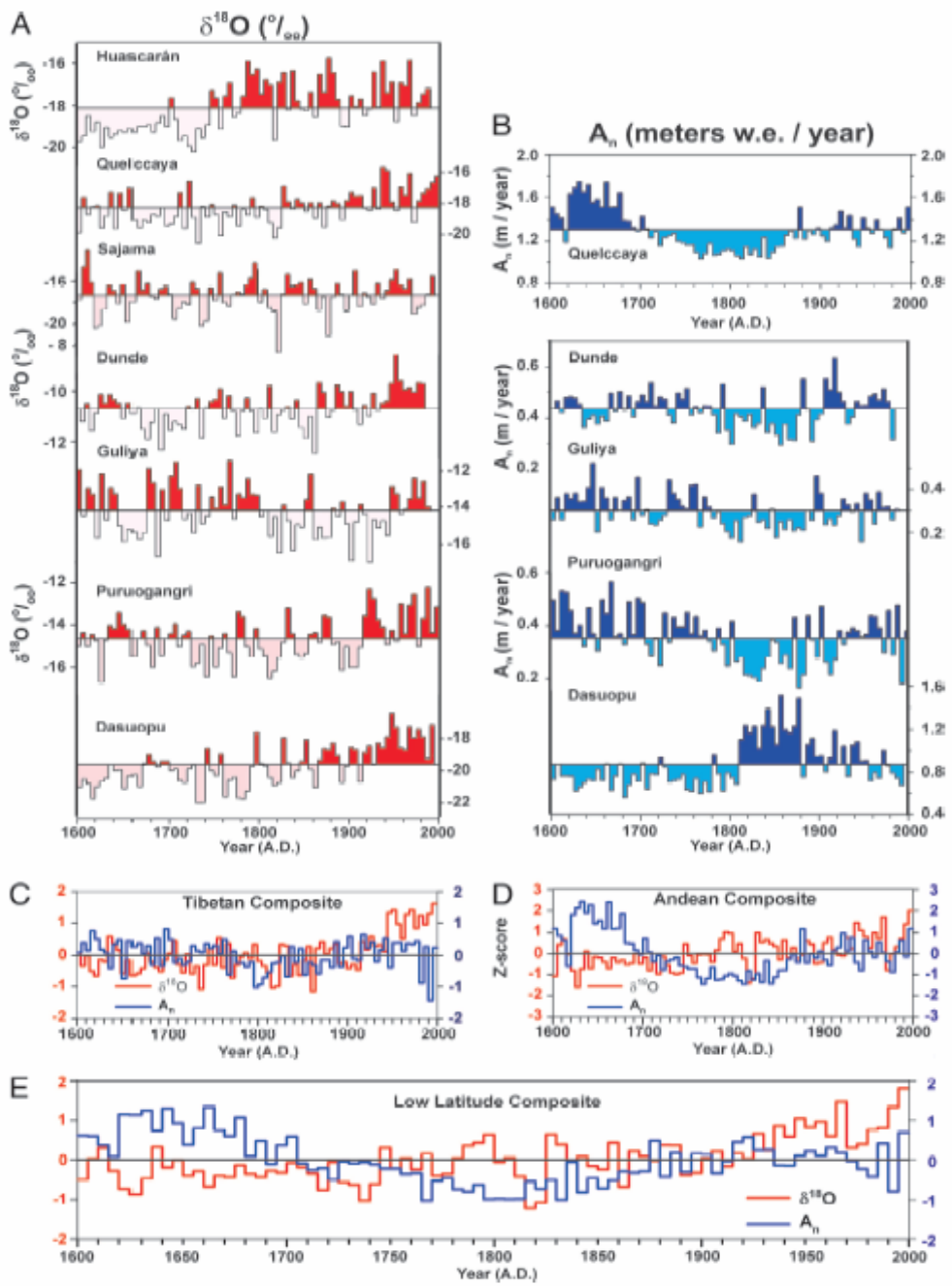

Figure 2: Climate reconstructions from 1600 – 2000. 5-year averages of $\delta^{18}O$ (A) and accumulation (B) for low-latitude ice cores. Accumulation is given in meters of water equivalent (w.e.) per year. Composite $\delta^{18}O$ and accumulation records for the Tibetan Plateau (C) and Andean (D) ice cores were combined to produce a low latitude composite (E). The composite records are shown as Z-scores. Thompson et al., 2006

2.2 Model Applications

Potential causes for past variations in the isotopic ratios of tropical ice cores can be determined using models with isotopic tracers. As isotopic variations become increasingly coupled to model physics (Schmidt et al., 2005a), models become more able to recreate past climates. Previous studies (Bradley et al., 2003; Francou et al., 2004; Schmidt et al., 2005b; Vuille et al., 2005) have both validated model output with isotopic proxy data, and also correlated proxy records with other aspects of the climate system. The effect of tropical sea surface temperatures on the Dasuopu ice core has been investigated using NCEP SST field (Bradley et al., 2003) to examine possible ENSO variability recorded in Himalayan ice cores.

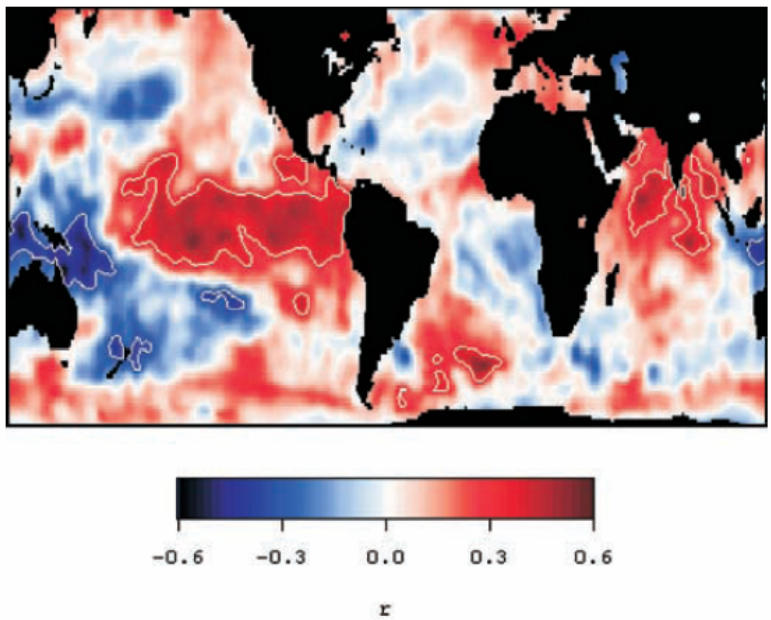

Figure 3: Correlation between the mean annual oxygen-isotope record in Dasuopu (cores 2 and 3) and June-September sea surface temperatures. The Dasoupu site is indicated with a white dot. White lines indicate areas within the 95% confidence interval (Bradley et al., 2004).

The Dasuopu $\delta^{18}O$ Core 3 record was compared to the ECHAM-4 T106 Atmospheric General Circulation Model (AGCM) with isotopic tracers to determine if the oxygen isotopes in Tibetan ice cores record the South Asian monsoon (Vuille et al., 2005). The oxygen-isotope record from the grid cell corresponding to the location of Dasuopu was used to both measure the internal consistency of the model as well as a comparison with the Dasuopu record itself. The grid cell and the Dasuopu data do not correlate ($r = 0.22$) (Vuille et al., 2005). Both the grid data and the Dasuopu $\delta^{18}O$ are negatively correlated with the chosen monsoon index. The definition of the monsoon index is the difference between the upper zonal

wind velocity anomalies during the months of June, July, August, and September (Webster and Yang, 1992).

Equation 1: $M = u_{850} - u_{250}$
M = Monsoon intensity
U850 = 850 hPa time-averaged wind anomalies across the monsoon region
U250 = 250 hPa time-averaged wind anomalies across the monsoon region
The monsoon region is 0º - 160ºE, 40ºN - 20ºS

The model remains internally consistent but is unable to reproduce high resolution data similar to the Dasuopu oxygen-isotope record (Vuille et al., 2005). Correlations of the Dasoupu $\delta^{18}O$ with NCEP-NCAR observed monsoon index, and with the ECHAM T106 gird cell against the ECHAM T106 monsoon index show that changes in monsoon strength are responsible for the majority of $\delta^{18}O$ variability in the Dasoupu ice core (Vuille et al., 2005).

3. METHODS

3.1 Model Description

The Goddard Institute for Space Studies (GISS) ModelE General Circulation Model (GCM) contains tracer submodules that allows for the use of dust and isotopes as tracers (Schmidt et al., 2005b). The M20 version of GISS ModelE is a 20-layer model with a horizontal resolution of 4º x 5º latitude by longitude. ModelE(M20) contains two extra surface and lower stratosphere layers, and four more layers above 10 hPa than the previous GISS model (Hansen et al., 2002; Schmidt et al., 2005). This increased vertical resolution and the addition of more isotopic and particulate tracers augment the ability to apply model output to paleoclimate proxy data.

Isotopes follow the phase changes and diffusion related to the cloud liquid vapor once every physics time step (30 minutes) in the model (Del Genio et al., 2005). A single grid box can contain both entraining and non-entraining convective plumes with tracers, and may also incorporate tracers in sea ice, soil layers, snow, rivers, or lakes (Schmidt et al., 2005). Modeled isotopic tracers mimic observations of deuterium and $\delta^{18}O$ from global International Atomic Energy Association and Global Network of Isotopes in Precipitation (IAEA GNIP) (Schmidt et al., 2005).

This study analyzes two transient runs forced with the observed sea surface temperature (SST) patterns for 1880-1994. GISS ModelE demonstrates El Niño –Southern Oscillation (ENSO) interannual

variability, and when observed SST forcings are applied, will reproduce the correct timing and magnitude for ENSO events (Figure 4). One run further incorporated the increased anthropogenic greenhouse gases, and will be referred to as the "forced run". The model run that keeps greenhouse gases at a pre-anthropogenic level will be considered the "unforced run". The model self-generates North Atlantic Oscillation (NAO) variability. The amplitude and impacts of the model NAO are similar to observational data, but the timing of the model NAO variability is uncorrelated to real world occurrences.

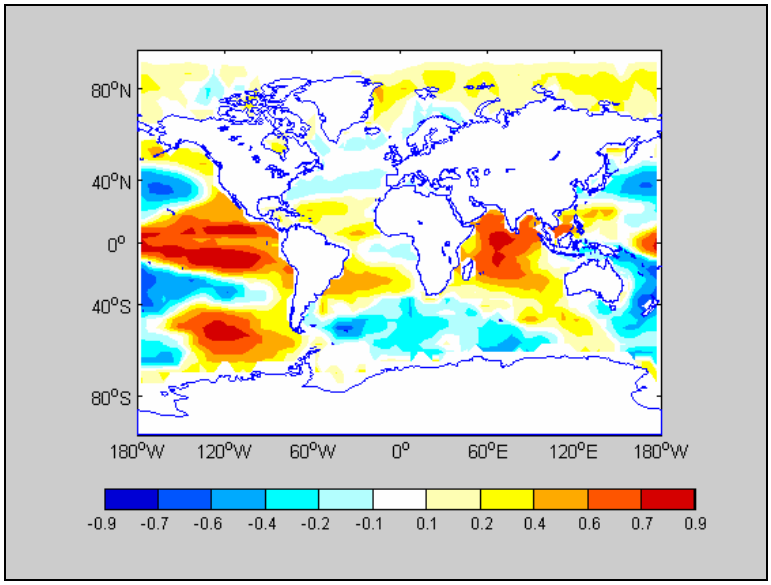

Figure 4: EOF1 of SSTs between 1880 – 1995, demonstrating the model's ability to recreate ENSO variability.

4. RESULTS

4.1 Monsoon Index

Webster and Yang's (1992) and Vuille et al's (2005) monsoon index as the domain-averaged difference in u_{850} and u_{250} hPa winds (Equation 1) was correlated with the Dasoupu data and the model output. Davis et al. (2005) separated the Dasuopu record into summer (JJAS) and winter precipitation (Figure 5). Only the proxy JJAS and model JJAS are examined from this point forward in order to mmore closely examine the monsoon months. The grid cell that encompasses Dasuopu, the grid cells directly to the west and east, and the three grid cells north of Dasuopu are used to analyze the model's simulation of oxygen isotopes in Dasuopu precipitation. This differs from other studies that only analyze the grid cell that corresponds with Dasuopu (Bradley et al., 2003; Vuille et al., 2005). Because of the model's coarse resolution, the grid box representing Dasuopu and its Himalayan neighbors have an elevation of 4000 m,

which averages the 8000 m peaks with their surrounding valleys. The grid boxes south of Dasuopu include the areas of heavy precipitation on the southern slope of the Himalayas and therefore are not an accurate representation of the climate processes affecting Dasuopu. The Dasuopu data, the unforced model run, and the forced run do not correlate with the monsoon index at the 95% confidence level, although the forced model run has the lowest p-value (0.0753) of the three (Figure 6). All three representations are positively correlated with the monsoon index, which opposes Vuille et al. (2005) who find significant negative correlations with the monsoon index.

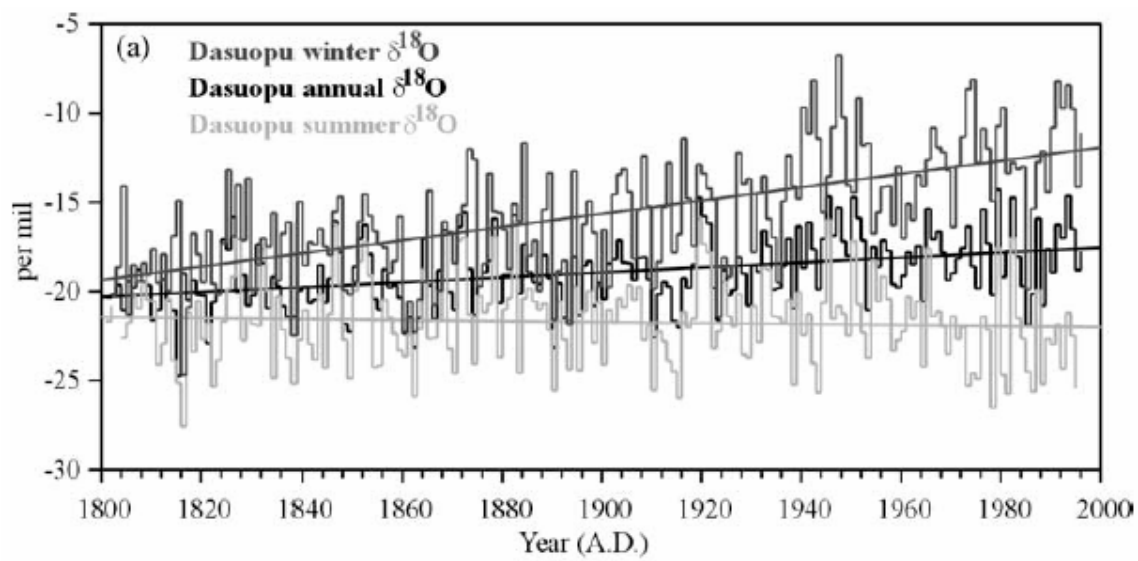

Figure 5: Time series of annual, winter, and summer seasonal values for the Dasuopu $\delta^{18}O$ (Davis et al., 2005). This study uses the same summer (JJAS) values for 1880 – 1995.

4.2 Westerlies Zonal Mean

Dasuopu's location at 30ºN and in the rainshadow of the Himalaya suggests that the westerlies may also affect the precipitation deposited on the ice cap. The westerlies have a documented impact on the ice cores collected from farther north on the Tibetan Plateau, and may have a slight effect on winter Dasuopu precipitation (Davis et al., 2005). The selection of only JJAS model and proxy data would suggest a negative correlation with the zonal mean of the westerlies. The zonal mean was defined as the difference between $u_{850}$and u_{250} global winds between 30ºN and 60º. Only the forced model data has a negative correlation coefficient with the westerlies zonal mean (-0.138). The forced and unforced model data, and measured Dasuopu data are not significantly correlated with the westerlies zonal mean (Figure 7).

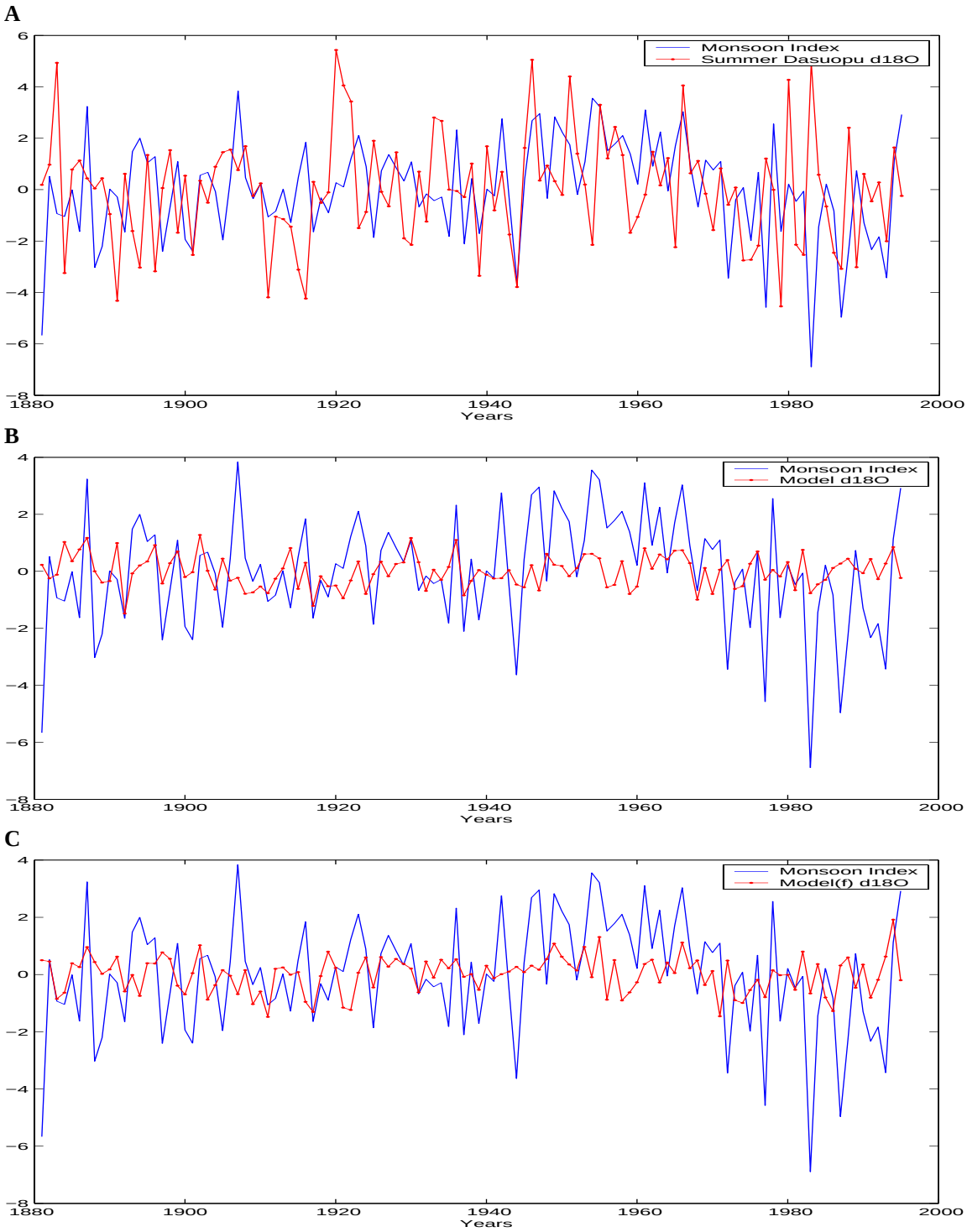

Figure 6: The detrended monsoon index compared to the precipitation-weighted JJAS Dasuopu $\delta^{18}O$, B) the detrended unforced model precipitation –weighted $\delta^{18}O$ for the six grid cells surrounding Dasuopu (details in text), and C) the forced model precipitation-weighted $\delta^{18}O$ for the same six grid cells. The p-values are 0.2543, 0.1694, and 0.0753 respectively, with N = 116, indicating the monsoon index is not significantly correlated to the oxygen isotopes in the Dasuopu core or in the model area surrounding Dasuopu.

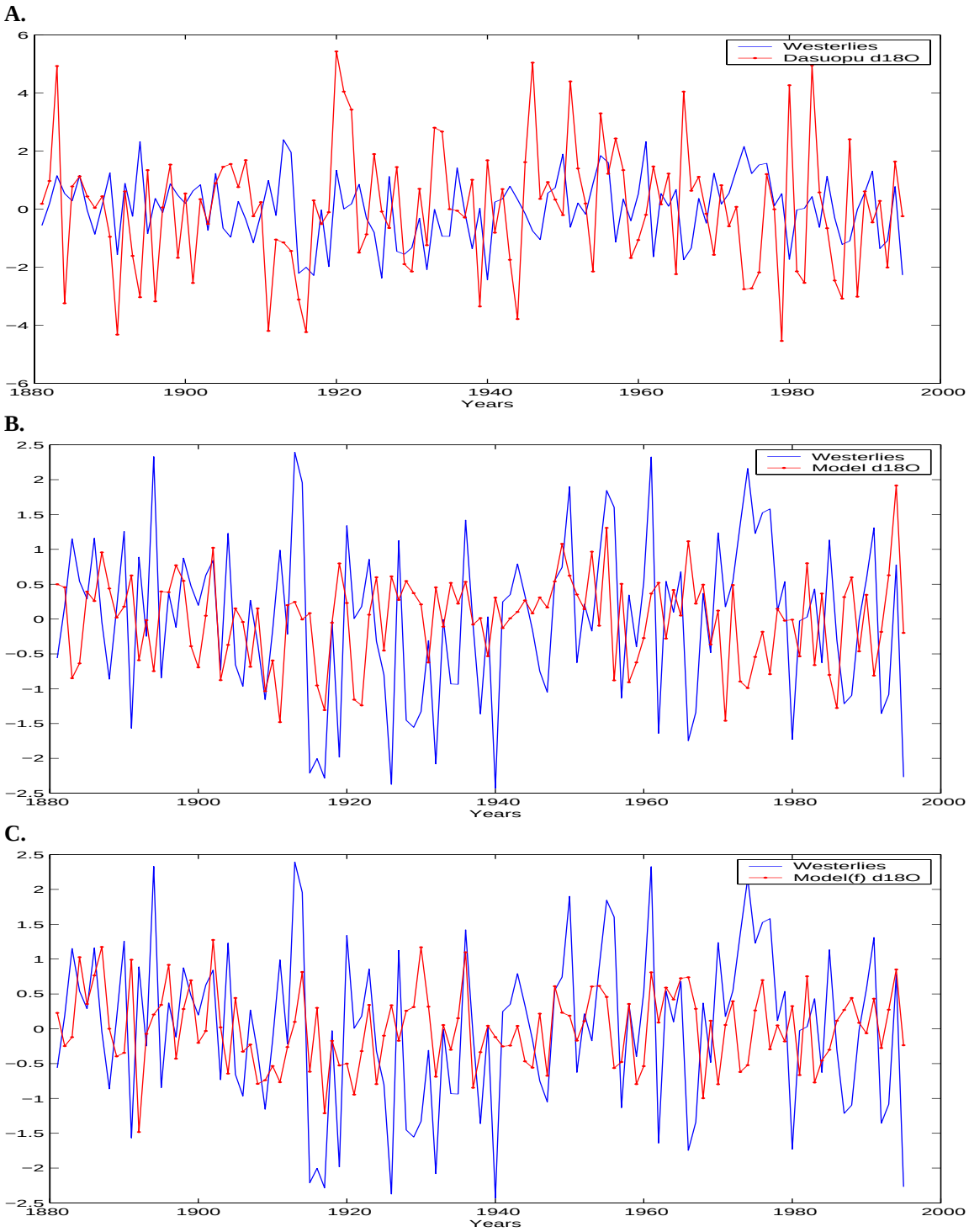

Figure 7: The detrended zonal mean of the westerlies compared to the precipitation-weighted JJAS Dasuopu $\delta^{18}O$, B) the detrended unforced model precipitation –weighted $\delta^{18}O$ for the six grid cells surrounding Dasuopu (details in text), and C) the forced model precipitation-weighted $\delta^{18}O$ for the same six grid cells. The p-values are 0.4101, 0.1553, and 0.3223 respectively, with N = 116, indicating the monsoon index is not significantly correlated to the oxygen isotopes in the Dasuopu core or in the model area surrounding Dasuopu.

4.3 Correlation Maps

In order to investigate the late Twentieth Century warming trend as recorded in tropical ice cores (Thompson et al., 2006), the Dasuopu $\delta^{18}O$ was correlated with surface air temperatures, sea surface temperatures, deuterium isotopes in water vapor at 500 hPa (the atmospheric level corresponding to Dasuopu), and ground temperatures between 1950 - 1995. The Dasuopu isotopic record was correlated both with the forced (Figure 8) and unforced (Figure 9) model runs. The ice core record strongly correlates with temperature (surface, ground, and SST) in the tropical west Pacific. This correlation does not extend to the north-western border of South America as depicted by Bradley et al., 2003. The use of NCEP-NCAR reanalysis data or the observational Niño 3.4 data set may serve as an intermediate comparison between the Dasuopu data and the model output. The correlation of Dasuopu with temperatures from the same region of the Pacific suggest that Tibetan ice cores may be recording changes in temperature on a greater than regional scale.

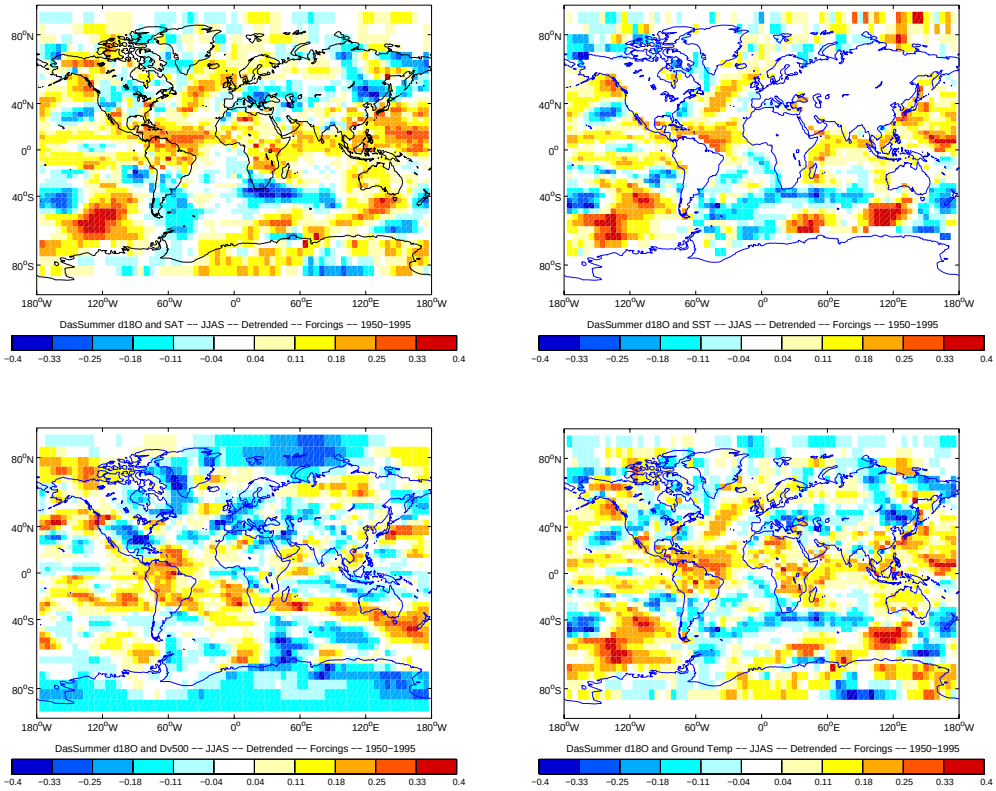

Figure 8: Correlation maps of detrended JJAS Dasuopu $\delta^{18}O$ with JJAS surface air temperature (top left), sea surface temperature (top right), deuterium in water vapor at 500 hPa (bottom left) and ground temperature (bottom right) for 1950 -1995. The strong correlations with the Southern Ocean may be a result of the model physics, and may show a more pronounced correlation than is present in observed data (G. Schmidt, personal communication).

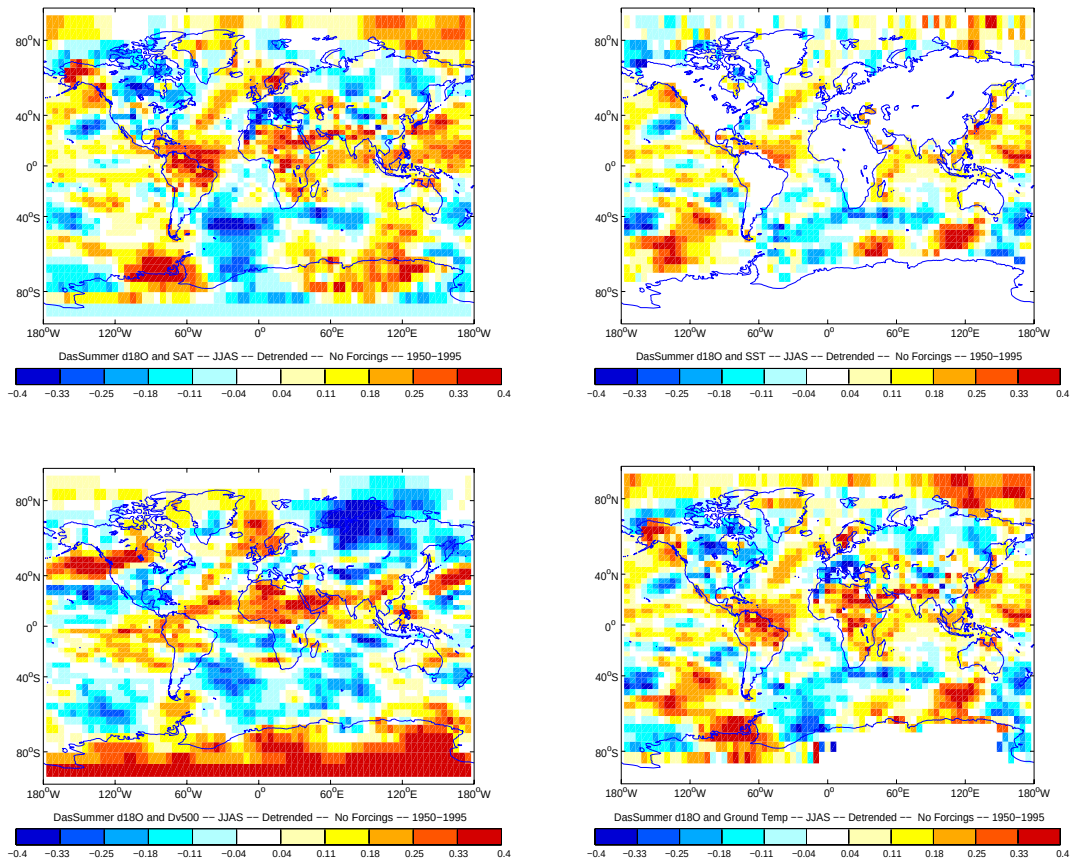

Figure 9: Correlation maps of detrended JJAS Dasuopu $\delta^{18}O$ with JJAS surface air temperature (top left), sea surface temperature (top right), deuterium in water vapor at 500 hPa (bottom left) and ground temperature (bottom right) for 1950 -1995. Model values are from the unforced run.

The correlations deuterium ratios at 500 hPa for both the forced and unforced model runs depict a latitudinal band of high correlation which may represent the convective precipitation of the intertropical convergence zone (ITCZ). In the unforced run (Figure 9) this band is located in the Northern Hemisphere, as would be expected for the months of June, July, August, and September. In the forced run, this latitudinal band is equally apparent (Figure 8), but is located in the Southern Hemisphere between 15º and 40ºS. The Southern Hemisphere location of the band of high correlation in JJAS would exclude it from being the ITCZ. The inclusion of increased greenhouse gases in the forced run significantly changes the global deuterium water vapor ratio.

5. CONCLUSION:

Comparing measured proxy data to models fitted with isotopic tracers provides an exciting opportunity to test the robustness of both data sets. Tropical ice cores are analyzed at a higher resolution and with more parameters than is possible with other proxy records. GISS ModelE currently contains the most sophisticated isotopic tracers in any general circulation model. This study presents an introductory example of the analyses that are possible by comparing high-resolution vertical proxy records with multiple parameters and spatial scale provided by the model. Integrating more ice core data or other proxy records will only serve to strengthen this type of analysis. The exponential retreat and disappearance of tropical ice caps increases the urgency to understand past changes in climate at these locations, and the natural and human-induced variability that can affect the livelihood of millions of people who depend on the water stored in the glaciers.

6. REFERENCES:

Bolzan, J. F. (1985). Ice Flow at the Dome-C Ice Divide Based on a Deep Temperature Profile. *Journal of Geophysical Research-Atmospheres* **90,** 8111-8124.

Bradley, R. S., Hardy, D., Thompson, L. G., and Vuille, M. (2003). Low latitude ice cores record Pacific sea surface temperatures. *Geophysical Research Letters* **30,** 4 p.

Davis, M. E., Thompson, L. G., Yao, T., and Wang, N. (2005). Forcing of the Asian monsoon on the Tibetan Plateau: Evidence from high-resolution ice core and tropical coral records. *Journal of Geophysical Research* **110,** 4101-4114.

Del Genio, A. D., Wolf, A. B., and Yao, M. S. (2005). Evaluation of regional cloud feedbacks using single-column models. *Journal of Geophysical Research-Atmospheres* **110**.

Francou, B., Vuille, M., Favier, V., and Caceres, B. (2004). New evidence for an ENSO impact on low-latitude glaciers: Antizana 15, Andes of Ecuador, 0 degrees 28 ' S. *Journal of Geophysical Research-Atmospheres* **109**.

Jones, P. D., New, M., Parker, D. E., Martin, S., and Rigor, I. G. (1999). Surface air temperature and its changes over the past 150 years. *Reviews of Geophysics* **37,** 173-199.

Schmidt, G. A., Hoffmann, G., Shindell, D. T., and Hu, Y. Y. (2005a). Modeling atmospheric stable water isotopes and the potential for constraining cloud processes and stratosphere-troposphere water exchange. *Journal of Geophysical Research-Atmospheres* **110**.

Schmidt, G. A., Ruedy, R., Hansen, J. E., Aleinov, I., Bell, N., Bauer, M., Bauer, S., Cairns, B., Canuto, V., Cheng, Y., DelGenio, A., Faluvegi, G., Friend, A. D., Hall, T. M., Yu, Y., Kelley, M., Kiang, N., Kock, D., Lacis, A., Lerner, J., Lo, K., Miller, R. L., Nazarenko, L., Oinas, V., Perlwitz, J., Perlwitz, J., Rind, D., Romanou, A., Russell, G. L., Sato, M., Shindell, D. T., Stone, P. H., Sun, S., Tausnev, N., Thresher, D., and Yao, M.-S. (2005b). Present day atmospheric simulations using GISS ModelE: Comparison to in-situ, satellite and reanalysis data. *Journal of Climate* **in press**.

Thompson, L. G., Davis, M. E., Mosley-Thompaon, E., Lin, P.-N., Henderson, K. A., and Mashiotta, T. A. (2005). Tropical ice core records: evidence for asynchronous glaciation on Milankovitch timescales. *Journal of Quaternary Science* **207,** 723-733.

Thompson, L. G., Davis, M. E., Mosley-Thompaon, E., Sowers, T. A., Henderson, K. A., Zagorodnov, V. S., Lin, P.-N., Mikhalenko, V. N., Campen, R. K., Bolzan, J. F., Cole-Dai, J., and Francou, B. (1998). A 25,000-year tropical climate history from Bolivian ice cores. *Science* **282,** 1858-1864.

Thompson, L. G., Mosley-Thompson, E., Brecher, H., Davis, M., Leon, B., Les, D., Lin, P. N., Mashiotta, T., and Mountain, K. (2006). Abrupt tropical climate change: Past and present. *Proceedings of the National Academy of Sciences of the United States of America* **103,** 10536-10543.

Thompson, L. G., Yao, T., Mosley-Thompaon, E., Davis, M. E., Henderson, K. A., and Lin, P.-N. (2000). A high-resolution millennial record of hte South Asian Monsoon from Himalayan ice cores. *Science* **289,** 1916-1919.

Vuille, M., Werner, M., Bradley, R. S., and Keimig, F. (2005). Stable isotopes in precipitation in the Asian monsoon region. *Journal of Geophysical Research-Atmospheres* **110**.

Webster, P. J., and Yang, S. (1992). Monsoon and Enso - Selectively Interactive Systems. *Quarterly Journal of the Royal Meteorological Society* **118,** 877-926.